Ceramics-Silikáty 65 (2), 198-205 (2021)
www.ceramics-silikaty.cz doi: 10.13168/cs.2021.0019

EFFECT OF Li_2O ON STRUCTURE AND PROPERTIES OF GLASS-CERAMIC BONDS

ZICHEN GUO, #FENG HE, ZUHAO LI, DONGYANG YAN, BING ZHANG, JUNLIN XIE

School of Materials Science and Engineering, Wuhan University of Technology, Wuhan 430070, China

#E-mail: he-feng2002@163.com

Submitted January 24, 2021; accepted February 26, 2021

Keywords: SiO_2–B_2O_3–Al_2O_3–CaO vitrified bonds, Glass-ceramics, Diamond, Sintering

SiO_2–B_2O_3–Al_2O_3–CaO vitrified bonds are widely used in the diamond abrasive tools preparation. The effect of Li_2O on structure and properties of the glass-ceramic bonds was investigated. The structure of the glass-ceramic bonds was analyzed by XRD and FTIR. The bending strength, the sintering properties of different glass-ceramic bonds and the thermal expansion coefficient were tested at meantime. The sintering and interfacial bonding state between L-4 glass-ceramic bonds and diamond grains were observed by SEM. The results showed that with the increasing of Li_2O, the sintering temperature of the glass-ceramic bonds was impactful reducing. When the content of Li_2O was 4 wt. %, the sintering temperature corresponding to the optimal bending strength was 630 °C, which had a certain reduction compared with other studies. The main crystal phase precipitated in the glass-ceramic bonds was $Li_xAl_xSi_{3-x}O_6$. With the increase of Li_2O, the number of crystals in the glass-ceramic bonds gradually increased. The highest bending strength could attain about 136 MPa. Meanwhile, the bending strength performed regular change as the rising of temperature accompanied by the linear shrinkage rate. The L-4 glass-ceramic bonds and diamond grains were found to have very good wetting property and the interfacial bonding strength was insured enhance. The average bending strength of the composite sinter of the glass-ceramic bonds and diamond was up to 87.8 MPa.

INTRODUCTION

Diamond is the hardest material in nature, which is often used to cut other materials. Diamond grinding wheels maintain mechanical properties through the combination of binding agents. Vitrified bonds diamond grinding wheels with excellent properties are widely used for grinding and machining materials [1-3], such as high strength, high elastic modulus, low fracture toughness, self-dressing, shape-retaining ability, high accuracy and low cost. These make high demands of diamond abrasive tools from high efficiency grinding to high precision grinding nowadays [4,5]. Vitrified bonds diamond grinding wheels are normally composed of three materials: diamond abrasive, filler and vitrified bonds. To some extent, the properties and qualities of diamond grinding wheels are determined by vitrified bonds. For diamond grinding wheels, oxidation may occur on surface during sintering. Therefore, two measures are often used. One is to use N_2 atmosphere to protect sintering, the other is to sinter at low temperature. At present, Chinese manufacturing enterprises are studying low temperature sintering mode without N_2 atmosphere protection. The sintering temperature of diamond grinding wheels mainly depends on the service temperature and content of binding agents. The researchers reduced the sintering temperature of diamond grinding wheels by reducing the sintering temperature of binding agents. SiO_2–B_2O_3–Al_2O_3–CaO vitrified bonds were often used as the basic system of diamond grinding wheels which had the properties of high bending strength and low softening temperature.

Zhao [6] reported that increasing Bi_2O_3 content decreased the thermal expansion coefficient of vitrified bonds, decreased the sintering temperature and improved their mechanical properties to some extent. Liu [7] suggested that Zr^{4+} could enter the glass network as mending nets and agglomeration composition, the addition of ZrO_2 increased the bending strength, crystallinity, sintering temperature of vitrified bonds and considerably decreased the wetting angle with diamond. The effect of other additives on the properties of vitrified bonds also had been investigated, such as titanium oxide [8], alkali oxides [9], alkali earth oxides [10]. However, only a few studies were reported on decreasing the sintering temperature and improving mechanical properties. Glass-ceramic bonds had demonstrated definite performance superiority compared with other vitrified bonds

system for the presence of microcrystal precipitated by controlled nucleation and crystallization of glass [11, 12]. The addition of Li_2O could reduce the melting temperature and increase mechanical strength of glass-ceramic bonds. Aiming at this target, there were two primary goals of this research. One was to increase the strength of glass-ceramic bonds and reduce the sintering temperature of glass-ceramic bonds. The evolution of structure and properties of glass-ceramic bonds was studied by changing the content of Li_2O and regulating the sintering system. The other was to ascertain the bonding state of diamond and glass-ceramic bonds for a better understanding of the microstructure of glass-ceramic bonds diamond grinding wheels.

EXPERIMENTAL

Preparation of glass-ceramic bonds

The chemical composition of glass-ceramic bonds was shown in Table 1. The parent glass was prepared by melting method, accurate weighing and mixing, and melting in a platinic crucible at 1450 °C for 2 h. Then the glass-frit was rapidly quenched in deionized water, dried, ball milled, and sieved to obtain the parent glass powders. The particle size range of powders was 2 - 5 μm. The mixed powders were pressed into the rectangular mould (45 × 6 × 6 mm) with an appropriate amount of 5 % PVA solution under a pressure of 25 kN. Finally, the compacted specimens were sintered under a certain heat treatment and cooled naturally in the muffle furnace in air atmosphere to prepare the glass-ceramic bonds.

Sample characterization

Phase structure and microstructure of glass-ceramics bonds

The crystalline phases were determined by XRD (D8 Advance, Bruker, Germany) equipped with a standard Cu Ka radiation source. The samples were scanned over a range of 2θ from 10° to 90° at a rate of 2° min^{-1}. FTIR measurement was carried out on a spectrometer (Nexus FT-IR, Thermo Nicolet, USA) in the range of 400 - 1600 cm^{-1}. The interface of the diamond grains and glass-ceramic bonds was observed by SEM (Japan, JMS-5610LV).

Performance of glass-ceramic bonds

Glass transition temperature (T_g) and crystallization temperature (T_c) were measured by DSC (STA 449 F1, Netzsch, Germany), operating at a heating rate of 10 °C·min^{-1} from room temperature to 800 °C in air. The bending strength of specimen was measured by three-point test method in the universal material tester (MTS810, MTS Co, USA) at a crosshead speed of 0.5 mm·min^{-1}.

RESULTS AND DISCUSSIONS

Effect of Li_2O on glass-ceramic bonds structures

Structural analysis of parent glass

The XRD pattern of parent glass with different Li_2O content was shown in Figure 1. It could be seen from the figure that there was no sharp diffraction peak in the pattern which was the typicality of amorphous state. The presence of a broad halo in between 15° and 35° indicated that parent glass was amorphous state and did not crystallize during melting at high temperature. The parent glass was mainly glass phase, which was conducive to the appearance of liquid phase during sintering and coating of diamond particle.

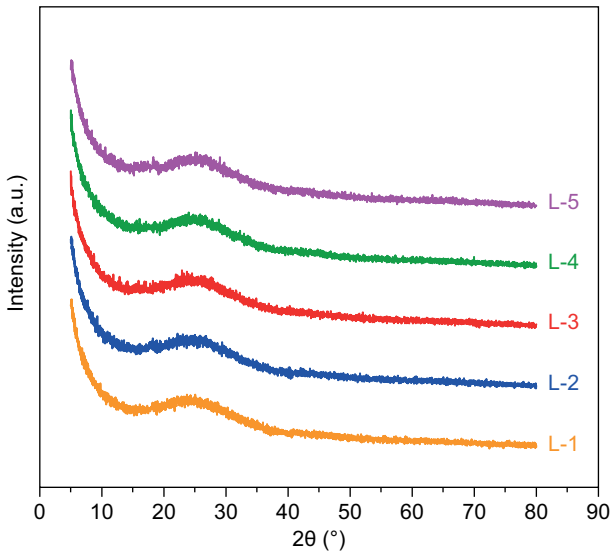

Figure 1. XRD pattern of parent glass with different Li_2O content.

Table 1. Chemical composition of glass-ceramic bonds (wt. %).

Sample ID	SiO_2	B_2O_3	CaO	Na_2O	Al_2O_3	BaO	Li_2O	Others
Li-1	60.00	10.00	10.00	5.00	5.00	2.00	1.00	7.00
Li-2	60.00	10.00	10.00	5.00	5.00	2.00	2.00	7.00
Li-3	60.00	10.00	10.00	5.00	5.00	2.00	3.00	7.00
Li-4	60.00	10.00	10.00	5.00	5.00	2.00	4.00	7.00
Li-5	60.00	10.00	10.00	5.00	5.00	2.00	5.00	7.00

The FTIR spectra of parent glass was shown in Figure 2. Five distinct absorption bands were observed in the FTIR spectra. It could be seen from figure that with the increase of Li_2O content, the main absorption bands of parent glass did not change, but the absorption vibration peak was affected.

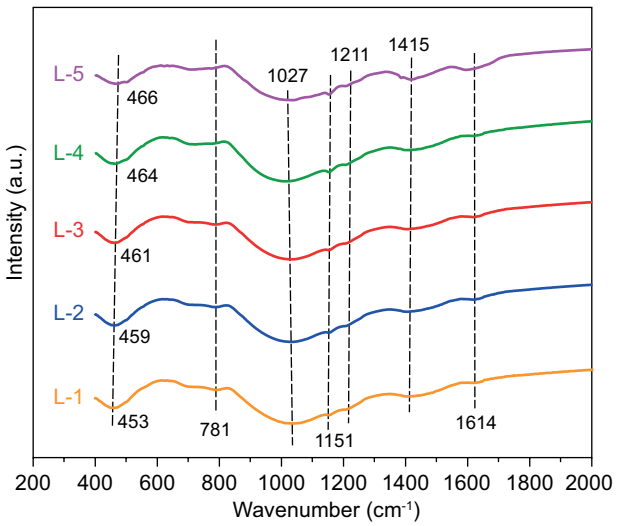

Figure 2. FTIR spectra of parent glass with different Li_2O content.

The parent glass exhibited IR band at around 461 cm^{-1} derived from bending vibration of O–Si–O in [SiO_4] [13]. The absorption peak around 790 cm^{-1} was symmetric stretching vibration of Si–O [14]. With the increase of Li_2O content, these two absorption peaks gradually weakened. That was because Li_2O played a role of breaking network structure, which could provide a large amount of free oxygen. The free oxygen would destroy the Si–O–Si structure, break the glass network structure, and change bridging oxygen to non-bridging oxygen, resulting in a reduction in the amount of [SiO_4]. Therefore, the Si–O–Si bending vibration peak and the symmetric stretching vibration peak of Si–O were weakened. The spectral band at 1027 cm^{-1} became narrower and split into three spectrum bands, 1027, 1151, and 1211 cm^{-1}. Wherein, the absorption peak around 1027 cm^{-1} was the result of combined effect of the asymmetric stretching vibration of Si–O–Si and the asymmetric stretching vibration of [BO_4] [15,16]. The characteristic bond of glass-ceramics appeared at 1151 cm^{-1}, and 1211 cm^{-1} was assigned to the asymmetric vibration of Si–O–Si [17]. With the increase of Li_2O content, the asymmetric stretching vibration of Si–O–Si tended to be obvious. The absorption peak around 1415 cm^{-1} was the asymmetric stretching vibration of [BO_3] [18], which gradually increased with the increase of Li_2O content. That was because in the glass system, [BO_4] and [BO_3] connected directly and the strength of B–O bond in [BO_3] was stronger than that in [BO_4]. The free oxygen introduced by Li_2O would reduce the amount of [BO_4] and increase the amount of [BO_3], which would cause the enhancement of the asymmetric stretching vibration of [BO_3] in the network structure, that was, the absorption peak at 1415 cm^{-1} gradually enhanced. It could be known from pattern that only the synergic absorption peak of the asymmetric stretching vibration of Si–O–Si and the asymmetric stretching vibration of [BO_4] appeared in the glass-ceramic bonds, but there was no the synergic absorption peak of [BO_3] and Si–O–Si bond. It indicated that in the glass network structure, the [SiO_4] was only connected to [BO_4], but not connected to [BO_3] and the [BO_3] was only connected to [BO_3] , indicating that the [BO_3] and the [BO_4] existed in a dense form, that was, there was a boron-rich phase, and the appearance of boron-rich phase would lead to another silicon-rich phase.

Thermal analysis of parent glass

The DSC curve of parent glass with different Li_2O content was shown in Figure 3. It could be seen from DSC curve that the obvious crystallization exothermic peak appeared from 500 °C. With the increase of Li_2O content, the peak temperature of crystallization exothermic peak gradually decreased from 536 °C to 526 °C. It indicated that with the increase of Li_2O content, the crystallization temperature shifted to low temperature, that was, the addition of Li_2O reduced the crystallization temperature. With the increase of Li_2O content, the area of crystallization exothermic peak gradually increased, that was, the number of crystals increased, indicating that the Li_2O promoted the precipitation of crystals. In addition, after the crystallization exothermic peak, the DSC curve showed a clear downward trend. That was because with the increase of temperature, the glass phase of parent glass gradually melted and the amount of liquid phase increased. The glass phase melting process was an endothermic process, so the DSC curve declined.

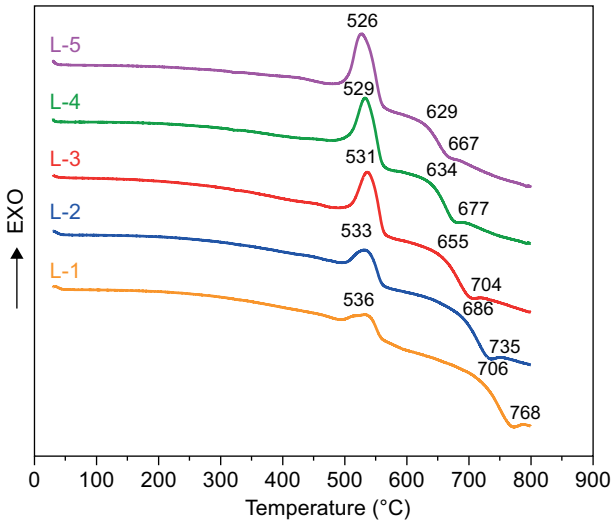

Figure 3. DSC curve of parent glass with different Li_2O content.

It could be known from thermal analysis results that the onset crystallization temperature of parent glass was around 500 °C. In order to achieve the best sintering, it was necessary to ensure appropriate amount of liquid phase to achieve the compact sintering of glass-ceramic bonds. The sintering temperature was set in the range of 590 - 720 °C, and a sintering temperature was taken every 10 °C. By adjusting the sintering temperature of each sample to control sintering and crystallization, the glass-ceramic bonds sintered body at different sintering temperatures was prepared.

XRD analysis of glass-ceramic bonds

The XRD pattern of glass-ceramic bonds sintered body with different Li_2O content at 660 °C was shown in Figure 4. According to the analysis of Jade 5.0 software, at the same sintering temperature, the crystal phases precipitated in the sintered body were all SiO_2 crystal, Al_2SiO_5 crystal and $Li_xAl_xSi_{3-x}O_6$ crystal. With the increase of Li_2O content, the intensity of diffraction peak of each crystal increased, indicating that the number of crystals increased and the crystals grew. When the content of Li_2O exceeded 4 %, the diffraction peak of crystal phase in the XRD pattern was particularly sharp and strong. That might cause the crystal grains to be too large, which would lead to the uneven structure of glass-ceramic bonds and the reduction of mechanical strength. The too many precipitations of crystal would also weaken the network structure and mechanical strength of glass phase, which affected the overall strength of glass-ceramic bonds [19].

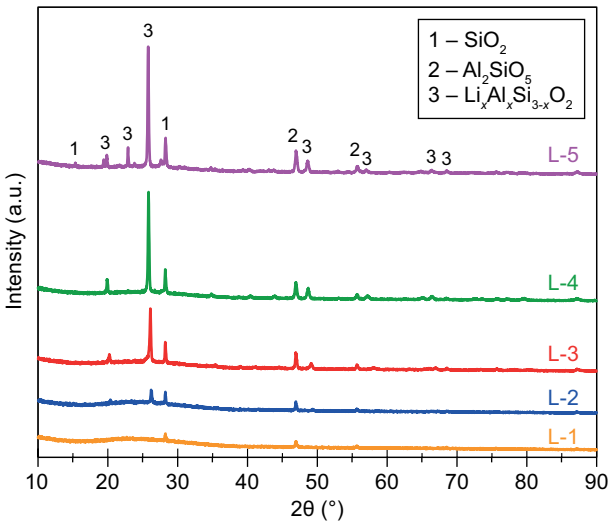

Figure 4. XRD pattern of glass-ceramic bonds with different Li_2O content at 660 °C.

In order to investigate the effect of sintering temperature on crystallization of glass-ceramic bonds sintered body, the XRD test was taken on the sintered body of L-4 glass-ceramic bonds at different sintering temperatures. The XRD pattern of L-4 glass-ceramic bonds sintered body at different sintering temperatures was shown in Figure 5. According to the analysis of Jade 5.0 software, at different sintering temperatures, the glass-ceramic bonds precipitated the same crystals, which were all SiO_2 crystal, Al_2SiO_5 crystal and $Li_xAl_xSi_{3-x}O_6$ crystal. It could be known from Figure 5 that with the increase of sintering temperature, the intensity of diffraction peak of crystal phase gradually increased and then remained unchanged. It indicated that with the increase of temperature, the type of crystal phase precipitated by glass-ceramic bonds was unchanged and the content of crystals increased and then remained unchanged. When the sintering temperature exceeded 630 °C, with the further increase of sintering temperature, the intensity of diffraction peak of crystal was unenhanced, indicating that in a certain composition, only increasing the sintering temperature within a certain temperature range could promote the precipitation of crystal.

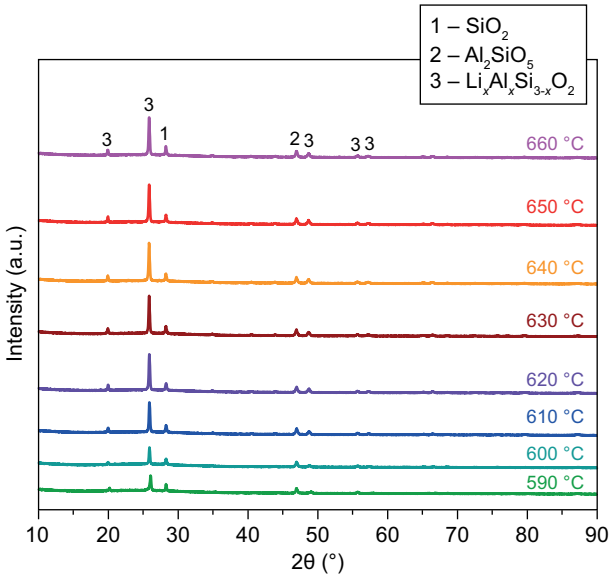

Figure 5. XRD pattern of L-4 glass-ceramic bonds at different sintering temperatures.

Micro-morphology analysis of glass-ceramic bonds

The micro-morphology of glass-ceramic bonds with different Li_2O content at 660 °C sintering temperature was shown in Figure 6. The distribution of glass phase and crystal phase in the glass-ceramic bonds could be seen from micro-morphology and the encapsulation effect of glass-ceramic bonds on diamond particle could be roughly predicted.

It could be known from Figure 6 that at this sintering temperature, the sintered body of each component was sintered densely, without a large number of obvious pores, but there were many thin pores. Li_2O could play a role of fluxing, that was, it had a function of lowering the

melting point and promoting the melting of glass phase. Therefore, at the same temperature, with the increase of Li_2O content, the content of liquid phase in the sintered body increased, and the fluidity was improved, which was conducive to promoting densification of sintering and reducing the porosity. An appropriate amount and evenly distributed micro-pores would be conducive to heat removal and chip removal of diamond grinding wheels during grinding process. At the same time, with the increase of Li_2O content, it could be seen from the figure that obvious regular crystals appeared, the number of crystals increased, and the grain size became larger. That was because Li_2O could promote the precipitation of crystal and the growth of crystal, and the appearance of an appropriate number of microcrystals would be conducive to improving the strength of glass-ceramic bonds.

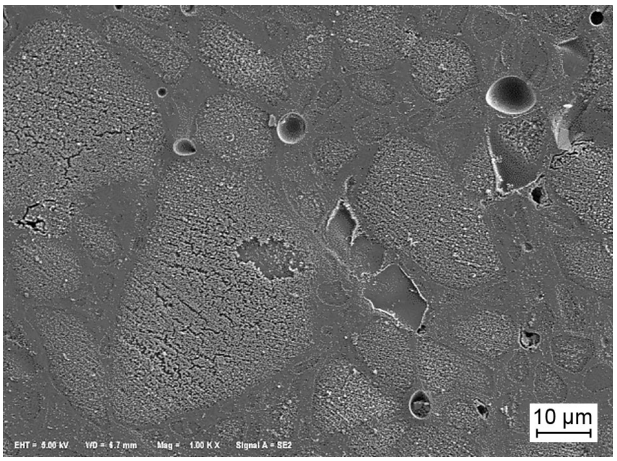

a) L-1

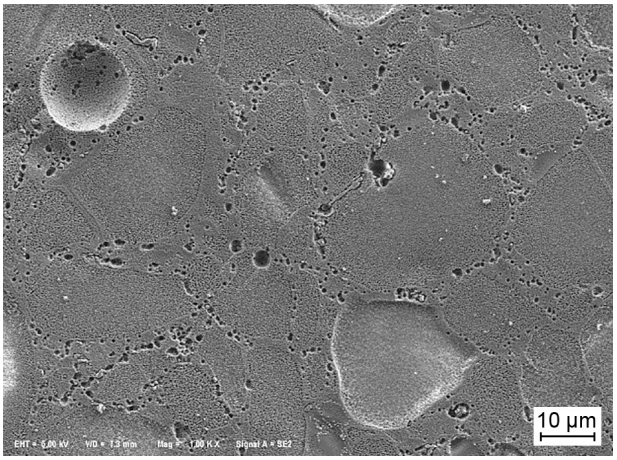

b) L-2

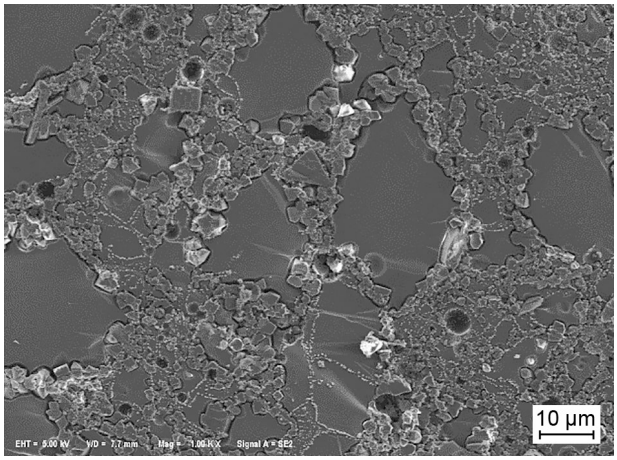

d) L-4

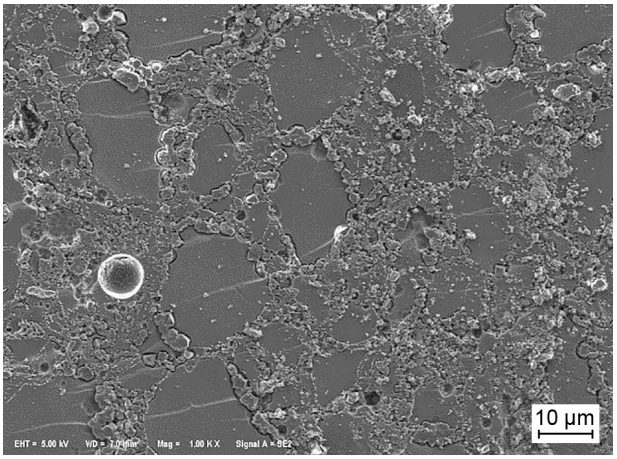

c) L-3

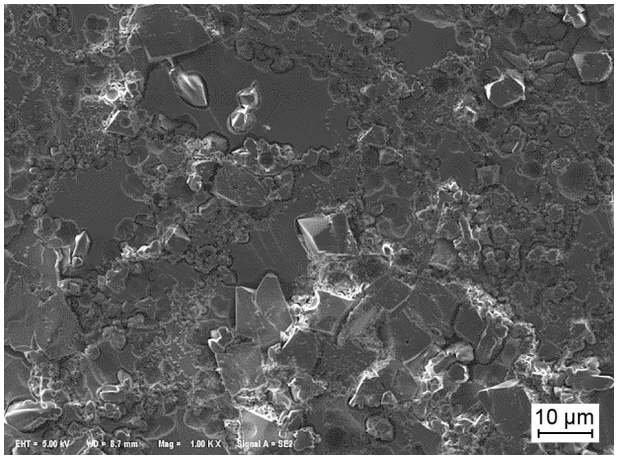

e) L-5

Figure 6. SEM of glass-ceramic bonds with different Li_2O content at 660 °C.

Effect of Li_2O on glass-ceramic bonds properties

Bending strength analysis

The performance of diamond grinding wheels was determined by bending strength of glass-ceramic bonds to a large extent. Therefore, improving the bending strength of glass-ceramic bonds was conducive to improving the performance of diamond grinding wheels. The bending strength curve of glass-ceramic bonds with different composition at different sintering temperatures was shown in

Figure 7. In the specific sintering temperature range, the bending strength of glass-ceramic bonds had the same variation trend as sintering temperature. It could be seen from curve that the bending strength increased with the increase of sintering temperature. After reaching the highest strength corresponding to sample, the sintering temperature continued to increase but the bending strength decreased. That was because the content of liquid phase changed with sintering temperature. The optimal sintering temperature of each sample was mainly affected by composition. With the increase of Li_2O content, the optimal sintering temperature of glass-ceramic bonds gradually decreased.

When the content of Li_2O increased to a certain extent, the maximum bending strength decreased instead. That was because in borosilicate glass, B atom could exist in the form of $[BO_3]$ in a chain or layer structure, which connection strength was low. B atom could also exist in the form of $[BO_4]$ tetrahedron, which had high connection strength. The two forms normally coexist in the glass network, but the relative content could be changed. The bonding interaction of Li_2O was weak. With the addition of Li_2O, a large amount of free oxygen was brought into glass network, and some $[BO_3]$ combined with free oxygen and changed to $[BO_4]$. In the glass-ceramic bonds system, $[BO_4]$, $[AlO_4]$ and $[SiO_4]$ constituted the main body of the three-dimensional network structure, and Li^+ could fill the network interspace as a network modifier. $[BO_4]$ had a higher network connection strength and a smaller volume than $[SiO_4]$. Therefore, the network structure formed by more $[BO_4]$ combining with $[AlO_4]$ and $[SiO_4]$ was denser and had better mechanical properties. However, when the content of Li_2O further increased, the excess free oxygen played a major role in breaking network. The free oxygen would form bond with Si atom, that was, the bridge oxygen bond in glass network was broken, and the glass network structure became loose, which had a significant fluxing effect, but it also reduced the bending strength of the glass-ceramic bonds. When the content of Li_2O was 4 wt. % and the sintering temperature was 630 °C, the glass-ceramic bonds exhibited the highest bending strength, which could reach 136 MPa.

Sintering shrinkage rate analysis

In order to investigate the sintering properties of different glass-ceramic bonds, the sintering shrinkage rate of samples were tested. In the sintering process, the phenomenon that the sample contracted in length or volume was called sintering shrinkage. Determining sintering shrinkage rate played an important role in choosing a reasonable glass-ceramic bonds. The linear shrinkage curve of glass-ceramic bonds with different component at different temperatures was shown in Figure 8. The changing law of curve was similar to the binding strength curve of glass-ceramic bonds with different component at different temperatures. That was, within a certain temperature range, the shrinkage rate increased first and then decreased. With the increase of Li_2O content, the maximum shrinkage rate increased, but when the content of Li_2O was too high, the maximum shrinkage rate decreased instead.

The consistency of changing law of linear shrinkage rate and bending strength indicated that the best bending strength meant the densest structure, that was, the greater the shrinkage of the glass-ceramic bonds was, the stronger the structure and the higher the strength was. The reason was also the change of liquid phase content of glass-ceramic bonds. With the increase of temperature, the content of liquid phase increased, the glass-ceramic bonds particles were easy to gather and sintered into entirety, and the gap between particles was conducive to the elimination of pores, so the linear shrinkage rate increased. When the sintering temperature was higher than optimal sintering temperature, the content of liquid phase was too much, the gap between particles was

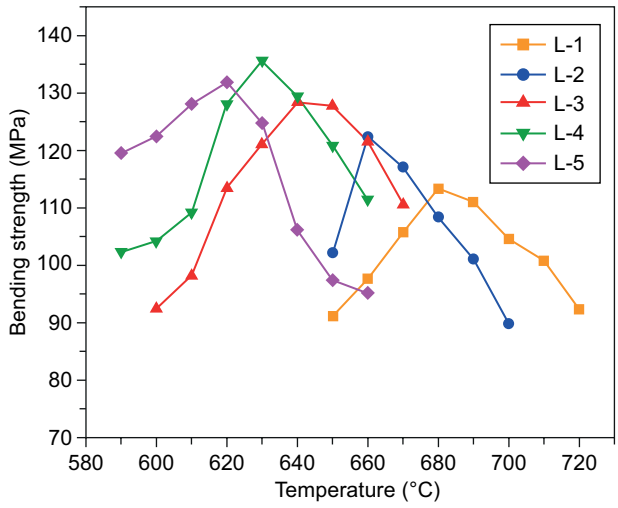

Figure 7. Bending strength of glass-ceramic bonds at different temperatures.

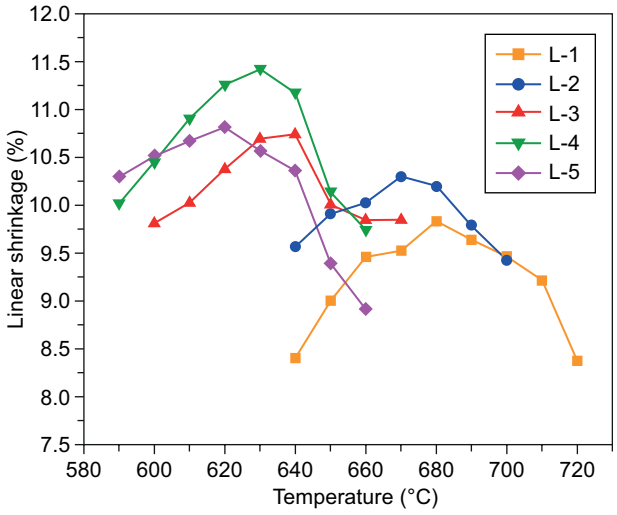

Figure 8. Linear shrinkage of glass-ceramic bonds with different content of Li_2O.

blocked, which was not conducive to the elimination of pores, so the linear shrinkage rate of glass-ceramic bonds decreased and the strength decreased. The above analysis indicated that to a certain extent, the change in linear shrinkage rate reflected the changing law of the strength.

Analysis of wettability and coverability

It could be known from the analysis of bending strength, sintering temperature and thermal expansion data that the maximum bending strength of L-4 glass-ceramic bonds at the sintering temperature of 630 °C was 136 MPa. It indicated that appropriate content of Li_2O played a great role in improving the comprehensive performance of glass-ceramic bonds. The L-4 glass-ceramic bonds with better comprehensive performance were chosen and sintered with diamond particles.

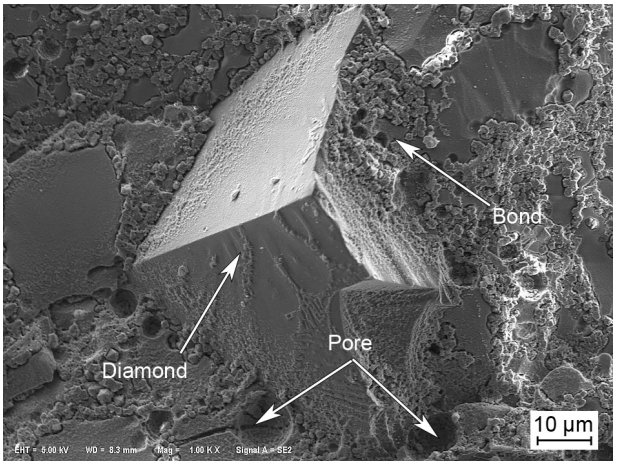

Figure 9. SEM of composite sinter of L-4 glass-ceramic bonds and diamond.

The SEM pattern of composite sinter of L-4 glass-ceramic bonds and diamond was shown in Figure 9. Wherein, the mass ratio of glass-ceramic bonds to diamond in composite sinter was 7:3, and the sintering temperature was 630 °C. It could be seen from pattern that the diamond particles were buried in glass-ceramic bonds, and were tightly wrapped by glass-ceramic bonds, indicating that the wettability and coverability of them were satisfactory. At the same time, it could also be seen that appropriate number of small grains were precipitated in the glass-ceramic bonds, which had a certain effect on improving the strength of composite sinter. The average bending strength of composite sinter was up to 87.8 MPa through the bending strength test, which was enough to meet the strength requirement of abrasive tools.

CONCLUSIONS

- With the increase of Li_2O content, the sintering temperature corresponding to the optimal bending strength of glass-ceramic bonds shifted to low temperature. When the content of Li_2O was 4 wt. %, the sintering temperature corresponding to the optimal bending strength was 630 °C.
- The main crystal phase precipitated in the glass-ceramic bonds was $Li_xAl_xSi_{3-x}O_6$, and the secondary crystal phase was SiO_2 and Al_2SiO_5. With the increase of Li_2O, the number of crystals in the glass-ceramic bonds gradually increased. When the content of Li_2O was 4 wt. %, the bending strength was 136 MPa, and the linear sintering shrinkage rate was 11.17 %.
- L-4 glass-ceramic bonds had a better wettability and coverability for diamond particles. The average bending strength of the composite sinter of the glass-ceramic bonds and diamond was up to 87.8 MPa.

Acknowledgement

The authors wish to express their sincere gratitude to Yumei Li, the Material Research and Testing Center of Wuhan University of technology.

REFERENCES

1. Han J., He F., Wang L. L., Zhang L. X., Ye C. Q., Xie J. L. et al. (2016): Effect of WO_3 on the structure and properties of low sintering temperature and high strength vitrified bonds. *Journal of Alloys and Compounds*, *679*, 54-58. doi: 10.1016/j.jallcom.2016.03.190
2. Hou Y. G., Qiao G. Y., Shang Y., Zou W. J., Xiao F. R., Liao B. (2012): Effect of porosity on the grinding performance of vitrified bond diamond wheels for grinding PCD blades. *Ceramics International*, *38*(8), 6215-6220. doi: 10.1016/j.ceramint.2012.04.074
3. He F., Zhou Q., Xie J. L., Zhang Q. P. (2015): Characterization of low sintering temperature and high strength SiO_2–B_2O_3–CaO vitrified bonds for diamond abrasive tools. *Ceramics International*, *41*(3), 3449-3455. doi: 10.1016/j.ceramint.2014.10.150
4. Xia P., Jiang R., Li Z., Zhu Y., Zhai C., Feng D., Sun, P. (2014): Effect of Y_2O_3 on the properties of vitrified bond and vitrified diamond composites. *Composites Part B: Engineering*, *67*, 515-520. doi: 10.1016/j.compositesb.2014.08.003
5. Kopac J., Krajnik P. (2006): High-performance grinding – a review. *Journal of Materials Processing Technology*, *175*(1-3), 278-284. doi: 10.1016/j.jmatprotec.2005.04.010
6. Zhao J., Zhu Y., Li Z., Lv X. (2013): Effect of Bi_2O_3 on physical properties of vitrified bond and mechanical properties of diamondcomposites. *Materials Science and Engineering: A*, *568*, 102-107. doi: 10.1016/j.msea.2012.12.067
7. Shang Y., Hou Y. G., Qiao G. Y., Zou W. J., Xiao F. R., Bo L. I. A. O. (2009): Effects of nano-AlN on phase transformation of low temperature vitrified bond during sintering process. *Transactions of Nonferrous Metals Society of China*, *19*, s706-s710. doi: 10.1016/S1003-6326(10)60136-7
8. Sun T., Xiao H., Cheng Y., Liu H. (2009): Effects of MO (MBa, Mg, Ca) on the crystallization of B_2O_3–Al_2O_3–SiO_2 glass-ceramics. *Ceramics International*, *35*(3), 1051-1055. doi: 10.1016/j.ceramint.2008.04.017

9. Shan D., Li Z., Zhu Y., Ye H., Gao K., Yu Y. (2012): Influence of TiO_2 on the physical properties of low-temperature ceramic vitrified bond and mechanical properties of CBN composites. *Ceramics International*, *38*(6), 4573-4578. doi: 10.1016/j.ceramint.2012.02.035
10. Aronne A., Depero L. E., Sigaev V. N., Pernice P., Bontempi E., Akimova O. V., Fanelli E. (2003): Structure and crystallization of potassium titanium phosphate glasses containing B_2O_3 and SiO_2. *Journal of Non-Crystalline solids*, *324*(3), 208-219. doi: 10.1016/S0022-3093(03)00263-1
11. Feng D., Zhu Y., Li F., Li Z. (2016): Influence investigation of CaF_2 on the LAS based glass-ceramics and the glass-ceramic/diamond composites. *Journal of the European Ceramic Society*, *36*(10), 2579-2585. doi: 10.1016/j.jeurceramsoc.2016.03.020
12. Shi J., H, F., Xie J., Liu X., Yang H. (2018): Effects of Na_2O/BaO ratio on the structure and the physical properties of low-temperature glass-ceramic vitrified bonds. *Ceramics International*, *44*(9), 10871-10877. doi: 10.1016/j.ceramint.2018.03.140
13. Efimov A. M. (1996): Quantitative IR spectroscopy: applications to studying glass structure and properties. *Journal of Non-Crystalline Solids*, *203*, 1-11. doi: 10.1016/0022-3093(96)00327-4
14. Doweidar H., El-Damrawi G., Al-Zaibani M. (2013): Distribution of species in Na_2O–CaO–B_2O_3 glasses as probed by FTIR. *Vibrational Spectroscopy*, *68*, 91-95. doi: 10.1016/j.vibspec.2013.05.015
15. Huang C., Behrman E. C. (1991): Structure and properties of calcium aluminosilicate glasses. *Journal of Non-Crystalline solids*, *128*(3), 310-321. doi: 10.1016/0022-3093(91)90468-L
16. Rao R. B., Gerhardt R. A. (2008): Effect of alkaline earth modifier ion on the optical, magnetic and electrical properties of lithium nickel borate glasses. *Materials Chemistry and Physics*, *112*(1), 186-197. doi: 10.1016/j.matchemphys.2008.05.046
17. Sales M., Alarcon J. (1995): Crystallization of sol-gel derived glass ceramic powders in the CaO–MgO–Al_2O_3–SiO_2 system. *Journal of Materials Science*, *30*(9), 2341-2347. doi: 10.1007/BF01184584
18. Shi J., He F., Xie J., Liu X., Yang H. (2019): Effect of heat treatments on the Li_2O–Al_2O_3–SiO_2–B_2O_3–BaO glass-ceramic bond and the glass-ceramic bond CBN grinding tools. *International Journal of Refractory Metals and Hard Materials*, *78*, 201-209. doi: 10.1016/j.ijrmhm.2018.09.015
19. Shi J., He F., Xie J., Liu, X., Yang H. (2018): Kinetic analysis of crystallization in Li_2O–Al_2O_3–SiO_2–B_2O_3–BaO glass-ceramics. *Journal of Non-Crystalline Solids*, *491*, 106-113. doi: 10.1016/j.jnoncrysol.2018.04.004